Anisotropic CSEM Inversion near the "Tiger" well in AC 818, Gulf of Mexico

Cam Kanhalangsy, Nick Golubev, Jurgen Johann Zach, Daniel Baltar, EMGS Americas*

Summary

We present anisotropic 2.5D inversion examples illustrating the possibility to image a resistor beneath gas hydrates with marine CSEM. The inversion examples are from a large CSEM survey conducted in 2008 in Alaminos Canyon, covering part of the Perdido fold belt. The focus of our study is on a part of the survey which is co-located with a recent partially published well, AC818-#1 ("Tiger"), and was acquired with very dense receiver spacing (0.5 km) and a source waveform with main frequencies of 0.5 Hz and higher. We show anisotropic CSEM inversion results for different background models. The resulting resistivity sections accurately recover the two most prominent features from the well independent of the assumed background model: shallow hydrates at the top of the Oligocene Frio sand as well as a high resistivity anomaly discovered in the Eocene Wilcox formation at the crest of the anticline. Both in terms of depth and structure, the CSEM, seismic and well log results agree well, even when the CSEM inversion is not constrained by a priori information in the form of seismic horizons.

Introduction

The Perdido Fold Belt is a large and prominent structure with northeast-southwest trending anticlines in the ultra-deep water (2.4 km – 3.2km) of the northwestern Gulf of Mexico. The area is characterized by concentric folds cored by autochthonous salt typically bounded by steep reverse faults. In Alaminos Canyon the fold belt consists of five parallel folds overlying north-east oriented basement highs, see figure 1 (Trudgill et al, 1999 and Fiduk et al., 1999). Petroleum prospectivity focuses on the crest of the anticlines as well as potential stratigraphic pinch-outs on the flanks. The most recent partially published well is AC, block 818 ("Tiger"; Latham et al., 2008; Boswell et al., 2009), drilled by Chevron in 2004. The focus of the latter is on the gas hydrate stability zone at less than 500 m burial depth as well as the crest of the Wilcox formation at about 800 m burial depth, both of which show increased resistive anomalies on the resistivity log. The hydrates penetrated by the "Tiger"-well are presumed to originate from deeper Eocene sands, and are located in the shallow regions of the Oligocene Frio sand uplifted during the late Oligocene compressional folding.

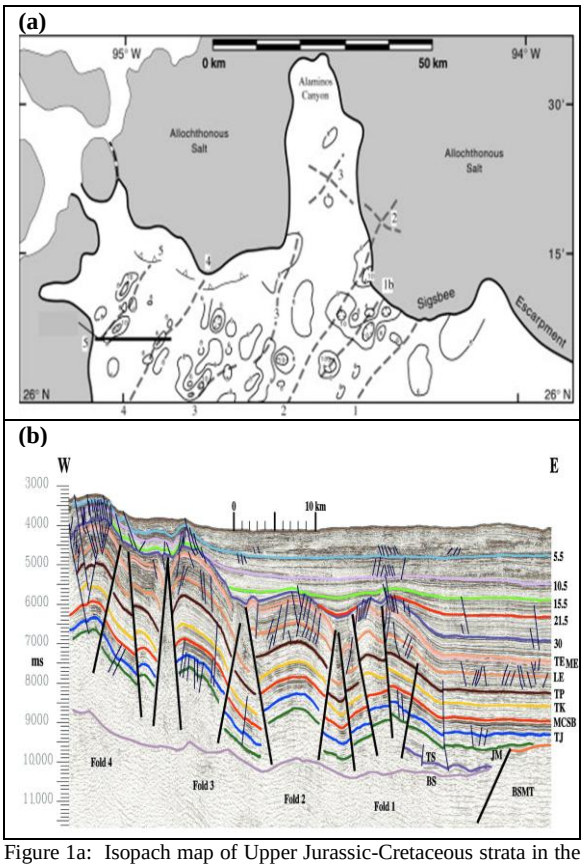

Figure 1a: Isopach map of Upper Jurassic-Cretaceous strata in the the Perdido fold belt (contour interval 2000 ft). The folds are numbered 1-5, anticlinal axes are shown by dashed lines. Figure 1b: interpreted W-E oriented regional seismic profile with some key horizons (e.g., T/M/LE: top/mid/lower Eocene, corresponding to ~3 km burial depth at the Eastern edge; BSMT: Basement). Sources: Trudgill et al, 1999 and Fiduk et al., 1999).

In June 2008, a marine CSEM survey was acquired with a base frequency of 0.2 Hz, covering about 1000 km^2 of the Alaminos Canyon, with a dense in-line receiver spacing of 0.5 km or 1 km and inter-line spacing of 4 km. This project was one of the first commercial, regional 3D CSEM scanning projects in the Gulf of Mexico. Part of the scanning area, see figure 2, was re-acquired with higher frequencies to better image the known shallow gas hydrate and the Wilcox discovery from the "Tiger' well in AC Block 818 (Latham et al., 2008).

The initial processing and interpretation of these data was performed using attribute displays and isotropic inversion. In 2010, the data were reprocessed using state of the art anisotropic inversion, better suited for this complex geologic environment. In this paper, we co-interpret CSEM line 02Tx003a inversion results with seismic and well data in the immediate vicinity of the "Tiger"-well, see figure 2. The source waveform was a periodic composite waveform with a base frequency of 0.5 Hz (see figure 3). All data

were inverted using anisotropic 2.5D CSEM inversion. Since the acquisition of azimuthal data was not the focus of the survey and due to the large inter-line spacing, the interpretation focused on 2.5D inversion instead of 3D inversion results.

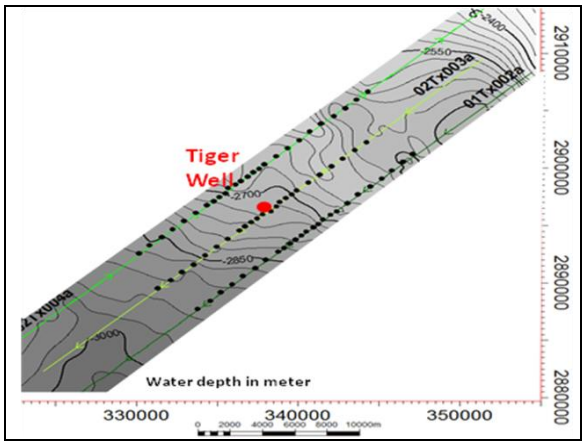

Figure 2. Survey design of the part of the Alaminos Canyon CSEM survey conducted in the vicinity of the "Tiger"-well with 1.0/0.5 km inline and 4.0 km inter-line spacing.

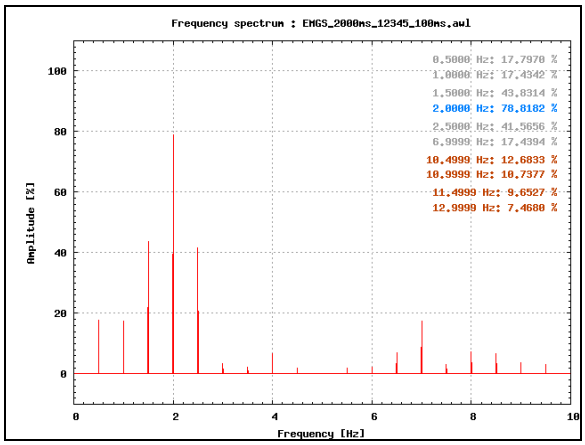

Figure 3. Source frequency spectrum with base frequency f_0=0.5 Hz.

Methodology

In order to tackle the non-uniqueness of inversion, our advanced processing methodology for marine CSEM data is based on an inversion strategy with increasing complexity, starting from plane-layer inversion of individual receivers to build background resistivity models for 2.5D and then 3D CSEM inversion, incorporating seismic & well data as available (see, e.g., Zach, 2010). The 2.5D inversion is based on full 3D modeling of the EM fields using the finite-difference time-domain solver described in Maaø, 2007, but with the assumption of transverse resistivity invariance. The forward modeling code runs on a regular simulation grid, which is remapped onto an arbitrary inversion parameterization. The update algorithm (described by Hansen and Mittet, 2009) centers on a Gauss-Newton algorithm with line search to minimize a cost function ε based on the L2 norm for data, summed over all receivers Rx, frequencies f and field components F:

$$\varepsilon = \sum_{Rx,f,F} \left| \text{Weight}(Rx, f, F) \cdot \left(F^{obs}_{Rx,f,F} - F^{syn}_{Rx,f,F} \right) \right|^2 + \lambda \varepsilon_{reg}, \quad (1)$$

where the regularization strength parameter weakens the regularization term $\lambda\varepsilon_{reg}$ during each iteration by typically a factor of 0.95 or greater. According to the geological problem investigated, the regularization term can be formulated with a great variety of constraints on the conductivity model σ, penalizing deviation from a priori models, spatial gradients, and other variations. In the present case study, we use the L1-norm of the deviation of the model gradient from an a priori model:

$$\varepsilon_{reg} = \sum_{i=x,y} \beta(x,z) \sum_{Rx,f,F} \left(\nabla_i \left(\sigma^{0.5}(x,z) \right) - \nabla_i^{AP} \left(\sigma^{0.5}(x,z) \right) \right)^2 \quad ,(2)$$

In practice, the a priori models used have constant resistivities within model layers with discontinuities across discrete seismic or other horizons favoring resistivity horizons.

Case study

As mentioned, the nearest CSEM line to the "Tiger" well is 02Tx003a with 24 receivers, at about 500 m distance (see figure 2). The water depth increases from about 2550 m at the northeastern end of the line to about 3000 m at the southwestern end of the line with moderately complex bathymetry. Concentrating on the shallow targets published in the well log by Boswell et al., 2009, relatively short-offset input data were used for the frequencies included with maximum offsets of {6 km, 5.5 km, 5 km, 4 km} for {0.5 Hz, 1.5 Hz, 2.0 Hz, 2.5 Hz}. Results of the 2.5D inversion of the inline electric field for 02Tx003a for two different start models are shown in figure 4 (half-space start model with ρ_v=2.25 Ωm and ρ_h=1.5 Ωm) and figure 5 (start model based on geologic horizons obtained through internal analysis; horizons were at the same time used as tear-surface discontinuities for the conductivity gradient).

Comparing figures 4 and 5 shows that the inversion is remarkably stable with respect to the start model especially in light of the complete absence of structural constraints in the half-space start model case. The vertical and horizontal resistivities, which are not explicitly constrained relative to each other, further indicate that the shallow hydrates and Wilcox target are thin resistors because they are not reconstructed in the horizontal resistivity image (Morten et al., 2010). The resistors in the CSEM inversion results occur approximately 100 m shallower than the gas hydrate and Wilcox discovery locations (Figure 6).

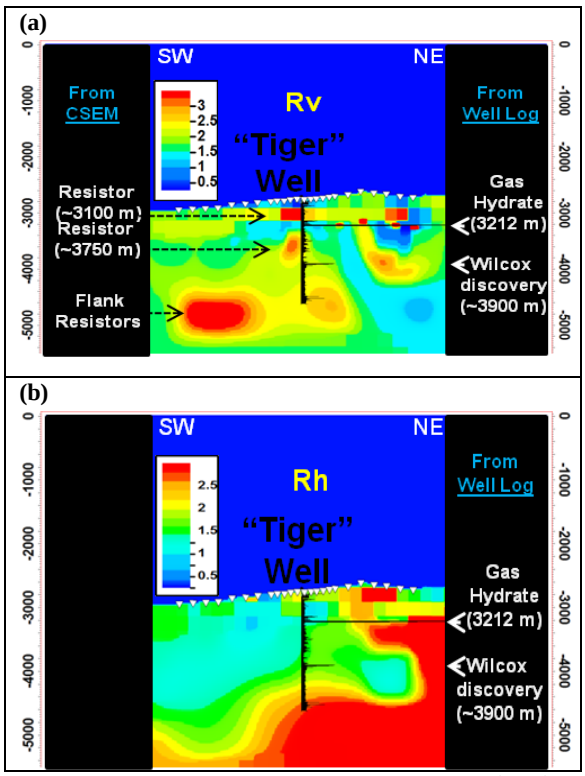

Figure 4. Vertical (a) and Horizontal (b) resistivity profiles from inverted CSEM line 02Tx003a superimposed with the “Tiger” well log resistivity column from a half-space start model.

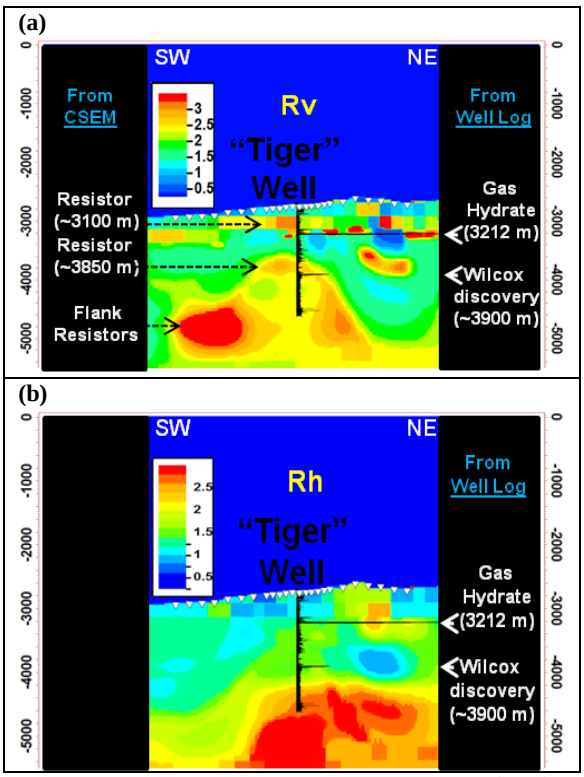

Figure 5. Vertical (a) and Horizontal (b) resistivity profiles from inverted CSEM line 02Tx003a superimposed with the “Tiger” well log resistivity column from a start and a priori model based on geological horizons.

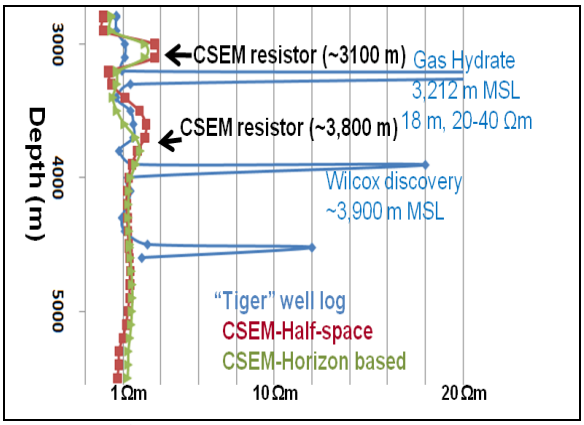

Figure 6. “Tiger” well log resistivity and extracted vertical resistivity columns from inverted CSEM line 02Tx003a near the “Tiger” well. Well log resistivity was up-scaled to 100 m intervals assuming serial coupling and an anisotrophy factor of 1.5. Gas hydrate depth of location, thickness and resistivity values are from Latham et. al, (2008).

The CSEM results exhibit high levels of depth consistency with seismic and log interpretations of the gas hydrate and the Eocene Wilcox discovery. In addition, the results

clearly indicate the anticline structure below the 'Tiger' well (figure 7 and figures 4 and 5). The benchmark data misfit for the final result of 2.5D CSEM inversion, 10% or less for most receivers and offsets, is met for both inversion runs (figure 8). The quality of the misfit is representative for all frequencies used.

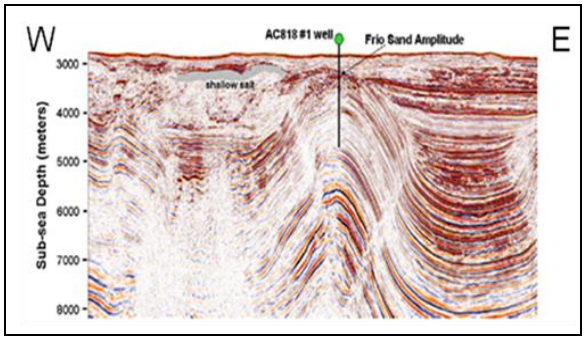

Figure 7. West-east trending seismic section across the AC 818 #1 ("Tiger") well showing the anticline structure (Source: Boswell et al., 2009). "Tiger" well is about 500 m north of CSEM line 02Tx003a.

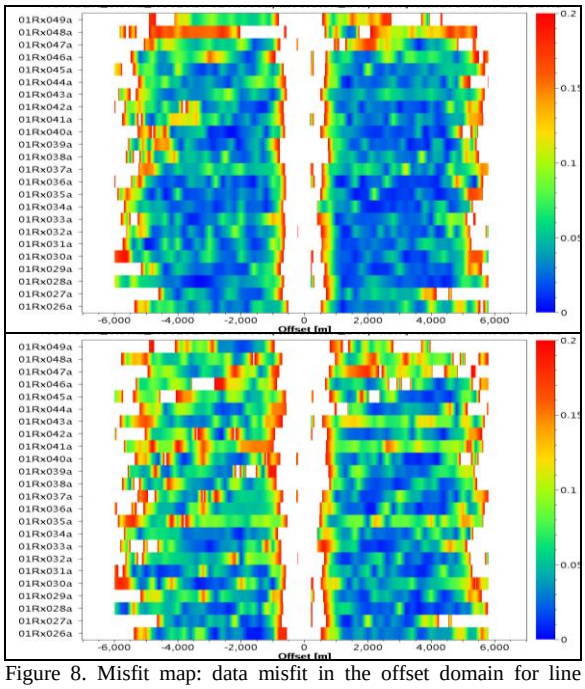

Figure 8. Misfit map: data misfit in the offset domain for line 02Tx003a for all receivers (each horizontal line represents one receiver) and a frequency of 2.0 Hz. Top: halfspace start model. Bottom: geology-based start and a priori model.

Conclusion

Anisotropic CSEM inversion was performed near the AC 818 well #1 ("Tiger"). The obtained subsurface resistivity profiles indicate relatively shallow resistors at approximately 3100 m and 3800 m below MSL, which are highly consistent with the known gas hydrate level (~3212 m below MSL), as well as the Eocene Wilcox discovery (~3900 m below MSL) as described from well data. The inversion results exhibit an anticline structure which correlates well with published seismic sections even when no structural constraints are imposed. There are also indications of resistors at the flanks of the anticline. The inversion results are robust with regard to qualitatively different starting models used and illustrate the possibility to image a resistive target beneath gas hydrates with marine CSEM.

Acknowledgements

We would like to thank EMGS Multiclient Services in Houston, TX for the opportunity to present these data and as well as the crew of the SIEM Mollie for their high quality and safe acquisition of these data.

EDITED REFERENCES

Note: This reference list is a copy-edited version of the reference list submitted by the author. Reference lists for the 2011 SEG Technical Program Expanded Abstracts have been copy edited so that references provided with the online metadata for each paper will achieve a high degree of linking to cited sources that appear on the Web.

REFERENCES

Boswell, R., D. Shelander, M. Lee, T. Latham, T. Collett, G. Gilles, G. Moridis, M. Reagan, and G. Goldberg, 2009, Occurrence of gas hydrate in Oligocene Frio sand: Alaminos Canyon Block 818: Northern Gulf of Mexico: Marine and Petroleum Geology, **26**, 1499–1512.

Fiduk, J. C., P. Weimer, B. D. Trudgill, M. G. Rowan, P. E. Gale, R. L. Phair, B. E. Korn, G. R. Roberts, W. T. Gafford, R. S. Lowe, and T. A. Queffelec, 1999, The Perdido Fold Belt, northwestern deep Gulf of Mexico, Part 2: Seismic stratigraphy and petroleum systems: AAPG Bulletin, **83**, 578–612.

Hansen, K. R., and R. Mittet, 2009, Incorporating seismic horizons in inversion of CSEM data: 79th Annual International Meeting, SEG, Expanded Abstracts, 694–698.

Latham, T., D. Shelander, R. Boswell, T. Collett, and M. Lee, 2008, Subsurface characterization of the hydrate bearing sediments near Alaminos Canyon 818: Proceedings of the 6th International Conference on Gas Hydrates (ICGH 2008).

Maaø, F. A., 2007, Fast finite-difference time-domain modeling for marine-subsurface electromagnetic problems: Geophysics, **72**, no. 2, A19–A23. doi:10.1190/1.2434781

Morten, J. P., A. K. Bjorke, and A. K. Nguyen, 2010, Hydrocarbon reservoir thickness resolution in 3D CSEM anisotropic inversion: 80th Annual International Meeting, SEG, Expanded Abstracts, 599–603.

Trudgill, B. D., M. G. Rowan, J. C. Fiduk, P. Weimer, P. E. Gale, B. E. Korn, R. L. Phair, W. T. Gafford, G. R. Roberts, and S. W. Dobbs, 1999, The Perdido Fold Belt, northwestern deep Gulf of Mexico, Part 1: Structural geometry, evolution and regional implications: AAPG Bulletin, **83**, 88–113.

Zach, J. J., 2010, Using sequential inversion schemes with increasing complexity to tackle the controlled-source electromagnetic imaging problem: Progress in Electromagnetics Research Symposium Abstracts, 424.